XIV International Conference on Computational Plasticity. Fundamentals and Applications
COMPLAS XIV
E. Oñate, D.R.J. Owen, D. Peric & M. Chiumenti (Eds)

COMPUTATIONAL MODELLING OF VOID GROWTH IN SWELLED HYDROGELS

L. SIAD*, M. ELKOLLI† AND S.C. GANGLOFF*

* Biomatériaux et Inflammation en Site Osseux (BIOS)
Université de Reims
UFR Pharmacie, 1 rue du Maréchal Juin, 51100 Reims, France
e-mail: {larbi.siad,sophie.gangloff}@univ-reims.fr, web page: http://www.univ-reims.fr/

†Laboratoire PMA des Matériaux Polymériques Multiphasiques (LPMAMPM)
Université Ferhat Abbas Sétif-1
Faculté de Technologie, 19000 Sétif, Algérie
e-mail: elkolli@hotmail.com - Web page: http://www.univ-setif.dz

Key words: Gels, Microvoid Growth, Multiscale Simulation, Porous Polymeric Biomaterials, Swelling.

Abstract. The nature and the large notable distinguishing features of polymeric gels explain their pervasive use as biomaterials in both regenerative medicine and tissue engineering. With regard to their biocompatibility, their ability to withstand large deformation and their significant capacity of solvent absorption, these biomaterials are often selected owing to their versatile mechanical properties and especially the closeness to soft biological tissues, amongst others. A finite-strain theory for the study of the overall behaviour of a porous polymeric gel where microvoids are present is presented. The swollen polymeric gel is modeled as a two-component body composed of two incompressible components, namely, an elastic porous polymer imbibed with a solvant. The chemical equilibrium is assumed to be preponderate at the interface between the porous polymer and the environment where the chemical potential of the solvent is fixed. The initially dry porous polymer undergoes large deformation induced by absorption of a solvent from the environment and mechanical loading. In this paper an attempt is made towards obtaining an estimation of the macroscopic responses of the swollen porous polymer to prescribed proportional loadings. To this end, a two-level representation of the material at hand for which the Representative Volume Element (RVE) imbibed with a solvent is a simple axisymmetric cylinder composed of a homogeneous matrix surrounding a spherical void, is considered. The computational study addresses the situation where the RVE is subjected to prescribed axial and lateral overall stresses under conditions of constant overall stress triaxiality. For fixed values of the Flory-Huggins parameter and the nominal concentration of the solvent, the overall stress-strain behaviour of the RVE model, the influence of the initial porosity, and the prescribed stress triaxiality ratio have been outlined.

1 INTRODUCTION

Hydrogels are pervasive in biology and have been turned out to be nearly optimal for interfacing with dynamic systems. By way of illustration, they are used as biomaterials in order to enhance stem cell transplantation by addressing, in particular, the mechanical aspects associated with each stage of the transplantation process [1, 17]. The characteristic soft ability of these polymeric biomaterials makes them strongly resembling the extracellular matrix (ECM) which encapsulates cells in their native environment. Regarding tissue engineering, scaffolds made of hydrogels, just like ECM, act as a structural support and are able to accommodate biomechanical signals to control cell function and eventually their fate [13]. Nowadays, it is trite to claim that stem cells are known to respond to mechanical cues in their microenvironment by changing their morphology, dynamics, proliferation rate, migration speed, and differentiation potential [7, 27]. The physical process of mechanosensitivity is realized through the contact and adhesion between cells and their microenvironment.

Hydrogels, a cross-linked polymers immersed in water, are an interesting class of materials that are able to undergo significantly large deformation which can also be triggered by external stimuli through appropriate change of constituents [26]. Solvent molecules migrate in a gel by self-diffusion. When hydrogels are subjected to mechanical loadings or also when the chemical potential of the environment changes, the polymer chain network deforms and the solvent molecules migrate to reach the thermodynamic equilibrium [28]. This equilibrium is reached as soon as the chemical potential of the solvent equals to that in the external solution. The mechanical, thermodynamic and kinetic properties of various environmentally sensitive hydrogels have been modeled and analyzed to study the different interesting phenomena exhibited, namely the phase transition and instability during swelling [2, 6, 20]. The interaction of mechanics and absorption of a swelling solvent in polymeric gels encompasses many important phenomena like environmental stress cracking, phase transformations, and cavitation to quote few. Very useful and recent presentations of the subject, based on continuum theories, may be found in a series of publications [3, 6, 9, 8, 12, 20, 36, 39] and references cited therein.

Poor toughness of soft porous biomaterials may results in failure which is an issue of importance to both engineering and medical practice [23, 37, 4]. An understanding of failure mechanisms turns out to be crucial in the study of fracture of these biomaterials. Cavitation is an important failure mode in elastomeric materials which includes situations where failure is mediated by environmental factors. Because of its close connection with material failure inception, cavitation has received much attention from the materials and mechanics communities [4, 16, 18, 21, 25]. Physical evidence showed that sufficiently large tensile loads can induce the sudden appearance of internal microvoids in elastomeric solids. Gent and Lindley [18] considered cavitation as the result of unlimited elastic expansion of a pre-existing microvoid. They used the elastic theory of void inflation to successfully correlate the critical load for cavitation with the corresponding one necessary for the unbounded growth of a microvoid in

an infinite medium. These authors conducted experimental investigations showing that the critical load for cavitation was directly related to the elastic modulus. On the other hand, the occurrence of such instabilities can also be attributed to the growth of pre-existing defects into finite sizes. In Ball's approach [4] cavitation is the start of a traction-free void within a nonlinear elastic solid as the consequence of reaching a critical load. Reviews as well as further details dealing with cavitation can be found for example in [16, 21]. Pence and Tsai [35] have extended the Ball's approach to account for the absorption of a swelling solvent resulting in volumetric changes at a fixed degree of swelling. They concluded that a Treloar material [38] always supports cavitation under uniform swelling provided that the load is sufficiently large. Duda *et al.* [12, 11] have shown that there is a critical value for the interaction parameter χ below which a Treloar material does not support cavitation regardless of the magnitude of the load. In addition, Zimberlin *et al.* [41], using a syringe needle to prescribe an internally pressurized void within a gel material, have proposed a method named "cavitation rheology testing" allowing the determination of the local modulus of the gel material. From these very short comments regarding the quantitative prediction of the occurrence of cavitation in real soft materials, it can be kept in mind that fundamental problems dealing with this subject remain largely unresolved [30, 29].

In addition to this, let us mention briefly that the toughness of a material depends on the ability of the microstructure to dissipate energy without propagation of defects like initiated microvoids or cracks [23, 37]. Subsequently, the understanding of failure mechanisms would also provide insight and afterwards enhancement into the production of tissue-engineering scaffolds with properly appropriate architecture and tailored properties. Scaffolds can be designed as porous structure (sponges) or in forms of hydrogels. Sponges facilitate cell adhesion and the pore size variation affects cell adhesion, migration and deposition. Hydrogels support the transportation of cells and bioactive agents and can suspend cells in a three dimensional environment. Keeping the focus on the porosity, among the essential characteristics that ideal scaffolds should share in order to be successful are the following [33, 32, 31] : i) the scaffolds should have high permeability to enable adequate diffusion of nutrients for the cells and the removal of waste products; ii) the cell supports porosity should be sufficiently high to allow for the ingress of cells and provide the cells space to proliferate and form the ECM; iii) they should have a large surface area; and iv) the pore size should be fine-tuned to the cells type applied.

As regard overall properties, the presence of those microscopic defects can have drastic consequences at the macroscopic level. In this computational study, the growth of a small spherical void within a polymeric gel is viewed through the prism of micromechanics [10, 34, 14] and finite element analysis. A two-level representation of the material at hand is considered. The mesoscopic scale is treated through an axisymmetric representative volume element (RVE) composed of two phases: a homogeneous void free matrix and spherical void. The behaviour of the RVE is appropriately averaged to provide the so-called macroscopic behaviour of the material considered as homogeneous. The calculations are very similar to many earlier similar simulations,

the prototype of which is due to Koplik and Needleman [24]. The boundary conditions of the RVE are prescribed under proportional stressing in such a way that the isotropically invariant stress triaxiality keeps a constant prescribed value throughout the loading displacement controlled history. The paper is organized as follows. Following [6, 12, 20, 22, 35], a general framework for studying the uptake of a solvent by a polymeric elastic solid is summarized in Section 2 where the basic constitutive equations are recollected. A brief presentation of the multiscale analysis and the description of the RVE model for the considered material are introduced in Section 3. Some of the obtained numerical results are presented in Section 4. Finally, concluding remarks are given in Section 5.

2 Governing equations

The problem formulation and material modelling of hydrogels are briefly presented in this section. Closely following works in [6, 12, 20, 22, 35], the governing equations and corresponding boundary conditions for equilibrium swelling deformation of this material are described. They serve as the basis for the numerical studies presented in the subsequent sections.

2.1 Kinematics and balance equations of finite growth

Consider a hydrogel body (current state) of volume Ω enclosed by a surface Γ, subjected to body force, $\underline{\mathbf{b}}$, and surface traction, $\underline{\mathbf{t}}$. Due to immersion of the hydrogel body in a solvent environment of chemical potential μ (per solvent molecule), a transport of the solvent molecules occurs within Ω and across Γ. In addition, part of the surface Γ may be mechanically constrained (*e.g.*, bounded to a rigid body) and/or chemically isolated from the solvent. Due to large deformation, it is more appropriate to use nominal quantities referring to a reference state with fixed volume Ω_o and surface Γ_o. A generic material particle occupying position $\underline{\mathbf{X}}$ at the reference state moves to position $\underline{\mathbf{x}}(\underline{\mathbf{X}}, t)$ at the current state at time t. The deformation gradient tensor maps both reference states, namely,

$$F_{iK} = \frac{\partial x_i(\underline{\mathbf{X}}, t)}{\partial X_K} \quad \text{with} \quad J := \det \underline{\underline{\mathbf{F}}} > 0 \tag{1}$$

While the choice of the reference state is arbitrary in general, we choose the dry state of the hydrogel as the reference state in the present study. Such a choice is necessary for the use of a specific free energy function. However, let us mention from now that a numerical challenge has to be circumvented in finite element analysis by using an intermediate configuration for which $J \neq 1$. The equation of force balance in terms of the nominal stress $\underline{\underline{\mathbf{s}}}$ and boundary conditions can be set as follows

$$\frac{\partial s_{iK}(\underline{\mathbf{X}}, t)}{\partial X_K} + B_i(\underline{\mathbf{X}}, t) = 0 \quad \text{and} \quad \underline{\mathbf{X}} = \bar{\underline{\mathbf{X}}} \text{ or } s_{iK} N_K = \bar{T}_i^o \tag{2}$$

where $\bar{\underline{\mathbf{T}}}^o$ is traction per unit area of the reference surface with the unit outward normal $\underline{\mathbf{N}}$ and the barred quantities are prescribed. In the circumstance of absence of

any chemical reaction, the conservation of the number of injected small molecules at the chemical potential μ into the gel, in the vicinity of $\underline{\mathbf{X}}$, read

$$\frac{\partial C(\underline{\mathbf{X}},t)}{\partial t}+\frac{\partial J_K(\underline{\mathbf{X}},t)}{\partial X_k}=r(\underline{\mathbf{X}},t) \tag{3}$$

where r is the number of the small molecules per unit time injected into a volume element dV, $J\,N_K\,dA$ is the number of the small molecules per unit time crossing an element of area $\underline{\mathbf{N}}\,dA$, and C be the concentration of the solvent number. The polymers and the individual small molecules are assumed to be incompressible, which is reflected in the incompressibility condition

$$1+v\,C(\underline{\underline{\mathbf{F}}},C)=J \tag{4}$$

where v is the volume per small molecule and $v\,C$ is the volume of the small molecules in the gel divided by the volume of the dry polymers.

2.2 Constitutive equations

Standard reasoning in thermodynamics accounting for condition of molecular incompressibility through the use of a field of Lagrange multiplier Π results in (refer *e.g.*, [6, 19, 39] and also to above mentioned references)

$$s_{iK}=\frac{\partial W(\underline{\underline{\mathbf{F}}},C)}{\partial \underline{\underline{\mathbf{F}}}}-\Pi\,JH_{iK}\quad,\quad \mu=\frac{\partial W(\underline{\underline{\mathbf{F}}},C)}{\partial C}+\Pi\,v \tag{5}$$

where W is the free energy of the gel and $\underline{\underline{\mathbf{H}}}$ is the transpose of the inverse of the deformation gradient $\underline{\underline{\mathbf{F}}}$, , namely, $H_{iK}F_{iL}=\delta_{KL}$ and $H_{iK}F_{jK}=\delta_{ij}$ [1].

For the dissipation due to solvent migration, we can correlate the solvent flux, $\mathbf{J}$, to its driving force, the chemical potential gradient, as

$$\mathbf{J}=-\mathbf{M}\boldsymbol{\nabla}_{\mathrm{X}}\mu \tag{6}$$

The spatial differential operator $\boldsymbol{\nabla}_{\mathrm{X}}$ is taken with respect to the reference configuration. The kinetic tensor $\mathbf{M}$ may not be constant in general, but is all positively definite.

The choice of an explicit form of the free-energy function W for elastomers and soft tissues is a controversial problem. This choice is needed in order to solve the initial value problem under consideration. Following Flory and Rehner [15], W has the form $W(\underline{\underline{\mathbf{F}}},C)=W_s(\underline{\underline{\mathbf{F}}},C)+W_m(C)$ reflecting the stretching network of the polymers, W_s, and the mixing of the polymers and the small molecules, W_m. These two terms are taken to be

$$\begin{aligned} W_s(\underline{\underline{\mathbf{F}}},C) &= \frac{1}{2}\,NkT(F_{iK}F_{iK}-3-2\log J)\\ W_m(C) &= -\frac{kT}{v}\left[vC\log\left(1+\frac{1}{vC}\right)+\frac{\chi}{1+vC}\right] \end{aligned} \tag{7}$$

[1] Algebraic identity: $\dfrac{\partial\,(\det\mathbf{F})}{\partial F_{iK}}=\det\mathbf{F}H_{iK}$

where N is the number of polymer chains in the gel per unit volume of the dry polymers, v is the volume per solvent molecule, T is the absolute temperature, and k is the Boltzmann constant. The first term inside the bracket comes from the entropy of mixing, and the second from the enthalpy of mixing. The Flory interaction parameter χ is a dimensionless measure of the enthalpy of mixing, with representative values $\chi = 0 - 1.2$. For applications that prefer gels with large swelling ratios, materials with low χ values are used. The enthalpy of mixing motivates the small molecules to enter the gel if $\chi < 0$, but motivates the small molecules to leave the gel if $\chi > 0$. The chemical potential and stresses are normalized by kT and kT/v, respectively. The material properties of the hydrogel is fully determined by three parameters: NkT, $\frac{kT}{v}$, and χ. The first two combine to give one dimensionless parameter, Nv. It is well known that NkT defines the initial shear modulus of the polymer network, with the number N proportional to the crosslink density ρ_c,[39, 38]. A representative value of the volume per molecule is $v = 10^{-28}\,\mathrm{m}^3$. At room temperature, $kT = 4 \times 10^{-21}\,\mathrm{J}$ and $kT/v = 4 \times 10^{7}\,\mathrm{Pa}$. In the numerical examples below, we will take the values $Nv = 10^{-3}$ and $\chi = 1.2$. The normalized chemical potential is mimicked by a temperature-like variable, which is uniform in the polymeric gel, and is incremented as a loading parameter. The whole governing equations and the thorough approach have been implemented into Abaqus via a UHYPER subroutine. [20, 22, 40].

3 THE AXISYMMETRIC RVE MODEL

The voids are assumed to be uniformly distributed inside the matrix material as shown in Figure 1-a. Specifically, the position of these voids are presumed to form a hexagonal crystal lattice in such a way that the shape of the unit microstructure is a prism with hexagonal basis face with inner radius R_o, height $2\,L_o$, and containing an initially spherical void with radius r_o. In order to reduce the effort of calculations to a two-dimensional analysis, the cross section of the unit microstructure has been simplified as a cylinder, as done in [5, 24]. Due to this approximation, the axisymmetric RVE is shown in Figure 1-d for which a cylindrical reference coordinate system with radial coordinate R, circumferential angle Θ and axial coordinate Z is used for the analysis. In the initial undeformed configuration, the RVE model is a cylinder with diameter $2\,R_o$ and height $2\,L_o = 2\,R_o$ (for the sake of simplicity). The initial axisymmetric RVE geometry is then simply characterized by the initial void volume fraction f_o given by $f_o = \frac{2}{3}\left(\frac{r_o}{R_o}\right)^3$. The RVE model is assumed to be subjected to axisymmetric deformations with constant prescribed overall triaxiality so that all field quantities are independent of Θ.

As a consequence of the lattice periodicity all outer planes of the unit cell have to move as rigid planes in coordinate directions during the process of loading (Figure 2). The faces at $R = R_o$ and $Z = L_o$ will have a uniform normal displacements and their mutual orientations will be maintained. These requirements impose the RVE model to remain, during the finite strain deformation process, a cylinder which is

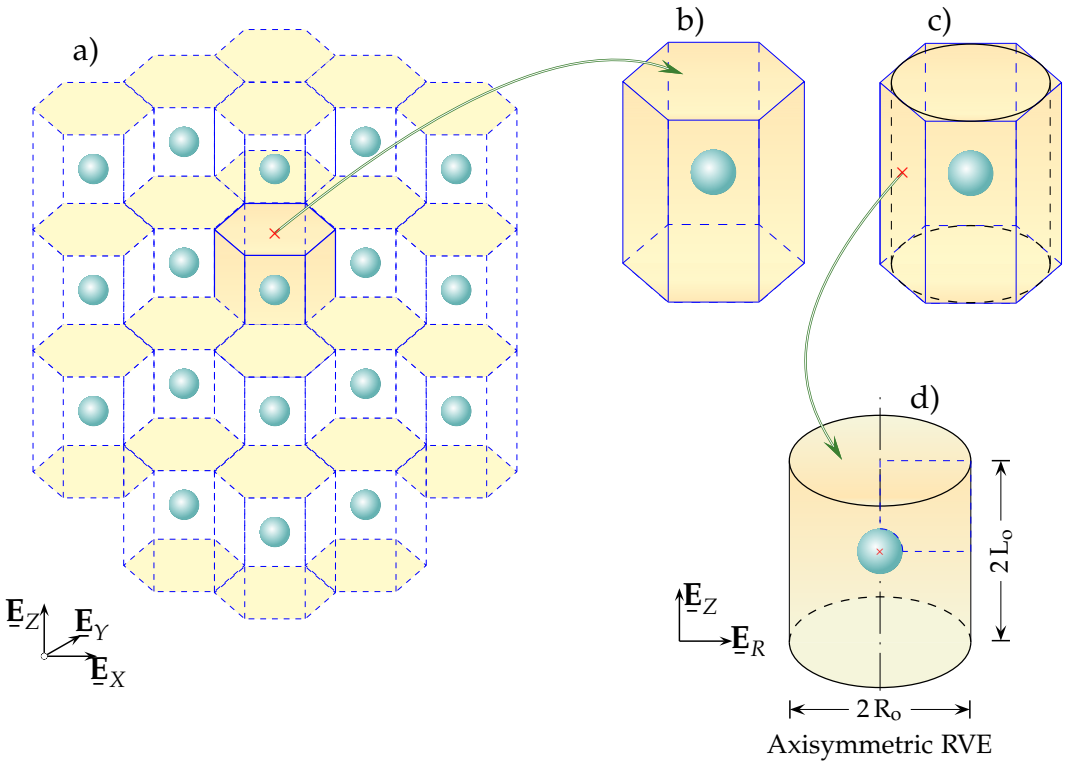

Figure 1: Three-dimensional hexagonal arrangement of spherical voids. a) Schematic representation of a porous polymeric gel which is considered as an array of unit hexagonal RVEs, each containing a single spherical void. The porous unit hexagonal microstructure shown in (b) is approximated by the axisymmetric RVE model displayed in (d).

thus characterized in an arbitrary state by $\ell_R = R_o + u_R^A$ and $\ell_Z = L_o + u_Z^A$ where u_R^A and u_Z^A are the radial and axial components displacement of the upper right corner **A**. Because of these constraints, only one quarter geometry of the RVE model ($0 \leq R \leq R_o$, $0 \leq Z \leq L_o$) needs to be analyzed and is drawn in Figure 2.

The overall deformation of the RVE model can be calculated from the normal displacements of the outer faces. The macroscopic total logarithmic strain tensor and Cauchy stress tensor possess the same principal directions, which are the radial and axial directions. The effective strain E_e defined by $E_e = \frac{2}{3}|E_Z - E_R|$ where E_R and E_Z are the macroscopic principal strains, is chosen as the overall deformation of the RVE model and the independent variable for presenting most results. The effective von Mises stress Σ_e , hydrostatic stress Σ_h, and the overall stress triaxiality $\mathcal{T}$ result from

$$\Sigma_e = |\Sigma_Z - \Sigma_R| \ , \ \Sigma_h = \frac{1}{3}(\Sigma_Z + 2\Sigma_R) \ , \ \mathcal{T} := \frac{\Sigma_h}{\Sigma_e} = \frac{1}{3}\frac{(\Sigma_Z + 2\Sigma_R)}{|\Sigma_Z - \Sigma_R|} \tag{8}$$

where Σ_R is the remote macroscopic principal stresses in both R and Θ directions, and Σ_Z in the Z-one. The RVE model is presumed to be remotely loaded with predominant axial stress; that is the axial direction is assumed to be the maximum prin-

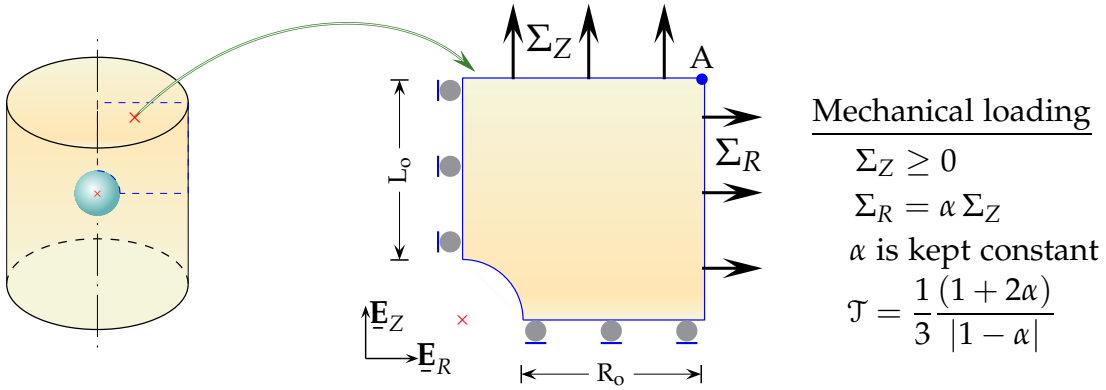

Figure 2: Axisymmetric RVE model containing an isolated spherical void and to be FE analyzed.

cipal direction and the components of the overall stress tensor $\underline{\underline{\Sigma}}$ are then such that $\Sigma_Z \geq \Sigma_R$.

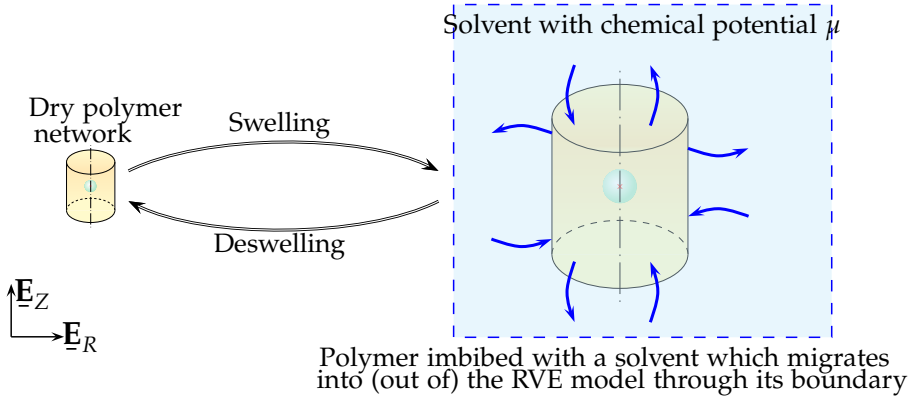

Figure 3: Swelling-deswelling of the axisymmetric RVE model. After swelling the porosity is maintained constant.

For metal, it is a well known fact that the stress triaxiality ratio $\mathcal{T}$ is the most important driving force to void growth in porous materials [5, 24]. On that account, a general problem in RVE model computations is to maintain $\mathcal{T}$ constant in the course of loading irrespective of the large displacement of the cell faces and the unstable stiffness behaviour. The finite elements used were eight-nodes quadrilateral isoparametric elements. The mesh surrounding the void is slightly refined and it was judged to be sufficiently refined for this study (800 Q8 elements). Care has been taken to insure that the meshes were sufficiently refined and that the results were independent of the degree of refinement. The Riks's arc-length method in Abaqus is used in order to handle the inevitable instability of the RVE and to proceed with further calculations. The overall stress and strain rates are directly computed from the reaction forces and the applied displacement rates. The actual void volume fraction f corresponding to

the evolution of the microvoid is calculated using numerical integration from the updated coordinates of the nodes at the void-matrix interface during the deformation of the RVE model. The initial conditions and loading rate of the RVE model are chosen such that inertial effects are negligible. No artificial damping has been used in all computations. The value of the imposed axial displacement u_z^A depends essentially upon the value of f_o and the fixed stress triaxility $\mathcal{T}$ as well. In addition, the imposed boundary conditions have to be ramped up using a function of time over the first part of calculation (typically the first 1-10%).

Before to proceed further, it is important to mention that the prevalent approach of modeling the porous biomaterial at hand as an assemblage of axisymmetric unit RVEs reduces the amount of work required for the multiscale analysis. This convenience comes with an approximation since this assemblage cannot patently fill the space continuously, and then is only suited for moderate porosity. Furthermore, the used axisymmetric RVEs do not allow the adjustment of arbitrary stress ratios in three directions.

4 NUMERICAL RESULTS

For the simulation presented hereafter, the chosen hydrogel properties are the following: initial polymer volume fraction $\phi_o = 0.90$, degree of cross-linking $N\nu = 0.0010$, and parameter $\chi = 0.10$. At the reference state corresponding to an initially swollen hydrogel of properties ϕ_o, $N\nu$ and χ, its initial chemical potential is prescribed by μ_o/kT given by $\mu_o/kT = N\nu(\phi_o^{1/3} - \phi_o) + \ln(1-\phi_o) + \phi_o + \chi\phi_o^2 = -1.3216$. This prescribed value is accounted for in Abaqus as an initial condition [40]. The porosity f_o takes on values $0.10, 0.50, 1.0, 2.0, 5.0$ and 10.0%. The stress triaxiality $\mathcal{T}$ ranges from $1/3$ (pure tension) to 2 (severe stress state for soft materials). However, in the interest of place, hereafter only the value $f_o = 5\%$ is considered.

The swelling-mechanical loading of the RVE model at hand may be summarised as follows: (a) the polymer network of the RVE model with initial porosity f_o is first imbibed with solvent as shown in Figure 3. Subsequently, homogeneous swelling occurs and the size of the RVE model changes a lot irrespective of the value of f_o. At equilibrium the chemical potential μ is homogeneous throughout the RVE model which porosity after swelling turns out to be practically equal to f_o. (b) The swelled RVE model is then subjected to axial and lateral overall stresses under conditions of constant prescribed overall stress triaxiality. Contour plots at the end of calculations of the lagrangian strain component LE_{22} are shown in Figure 4 for $\mathcal{T} = \frac{1}{3}, 1$ and 2. For each of these values of $\mathcal{T}$, the evolution of the normalized effective stress, $\frac{\Sigma_e}{kT}$ and the porosity f are displayed in Figure 5 as a function of the equivalent strain E_e.

It is to be noted that for moderate stress triaxiality (*e.g.*, $\mathcal{T} = \frac{1}{3}$ corresponding to a tensile test), the equivalent stress Σ_e continuously increases with equivalent strain E_e. The same applies to the variations of void volume fraction f in terms of E_e, (red curves in Figure 5). By way of example, it can be observed from Figure 5 that for $\mathcal{T} = 1$ (magenta curve) beyond the peak stress corresponding to $E_e = 0.39$, $(\frac{\Sigma_e}{kT})^{max} = 1.22 \times$

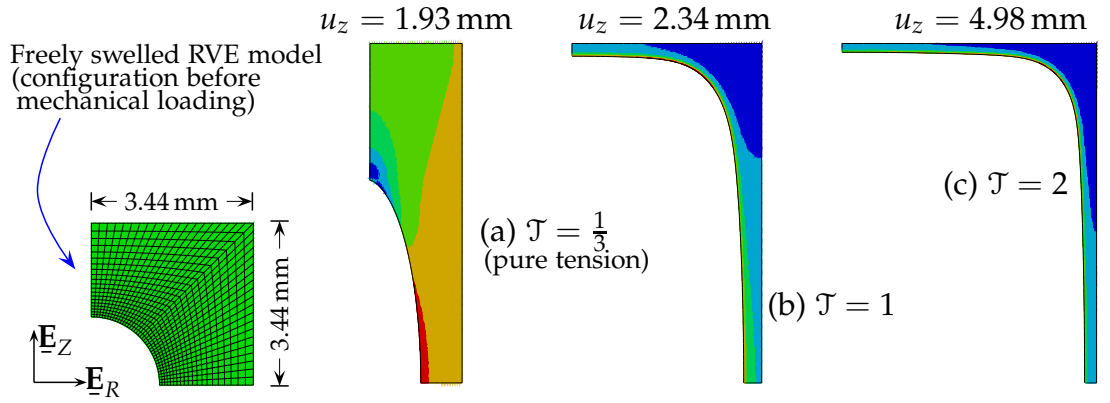

Figure 4: Distribution of lagrangian strain component LE_{22} at the end of calculations and final deformation shape of the RVE model for $f_o = 0.05$. The hydrogel properties are $\phi_o = 0.90$, $Nv = 0.0010$, and $\chi = 0.10$. The mechanical loading of the freely swelled RVE model has been performed under constant stress triaxiality ratio $\mathcal{T} = \frac{1}{3}$ (a), 1 (b), and 2 (c).

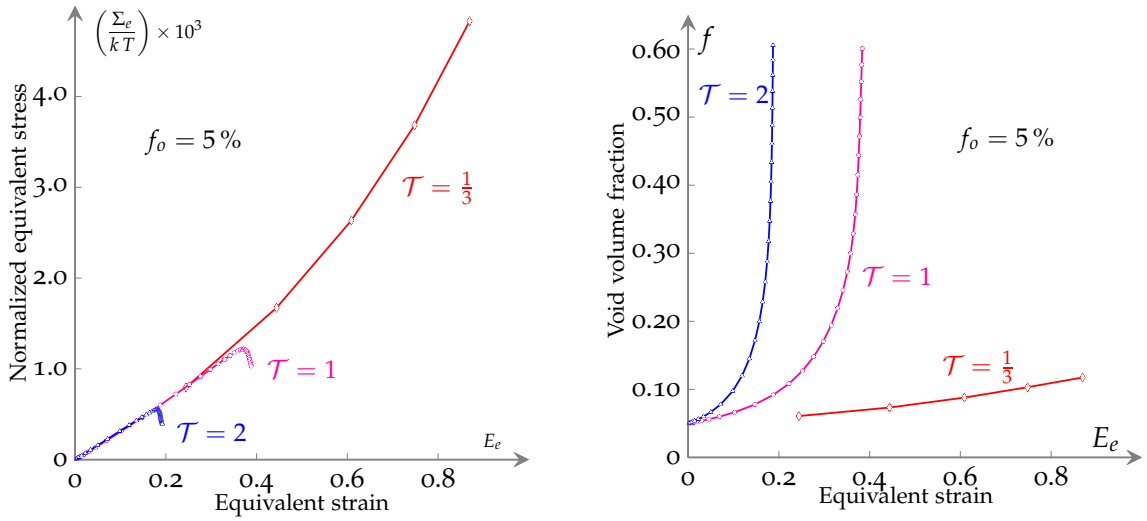

Figure 5: Evolution of the normalized equivalent stress $\frac{\Sigma_e}{kT}$ and the void volume fraction f in terms of the macroscopic equivalent strain E_e of the RVE model. The initial value of the void volume fraction is $f_o = 0.050$ and along the whole process of deformation the overall stress triaxiality $\mathcal{T}$ is kept constant.

10^{-3}, and $f = 38.6$ %, the void volume fraction increases very quickly. Figures 6–8 shows the deformation of the RVE model and the evolution during the whole process

of loading of the lagrangian strain component LE_{22} for $\mathcal{T} = 1/3$ (a), $\mathcal{T} = 1$ (b) and $\mathcal{T} = 2$ (c), respectively.

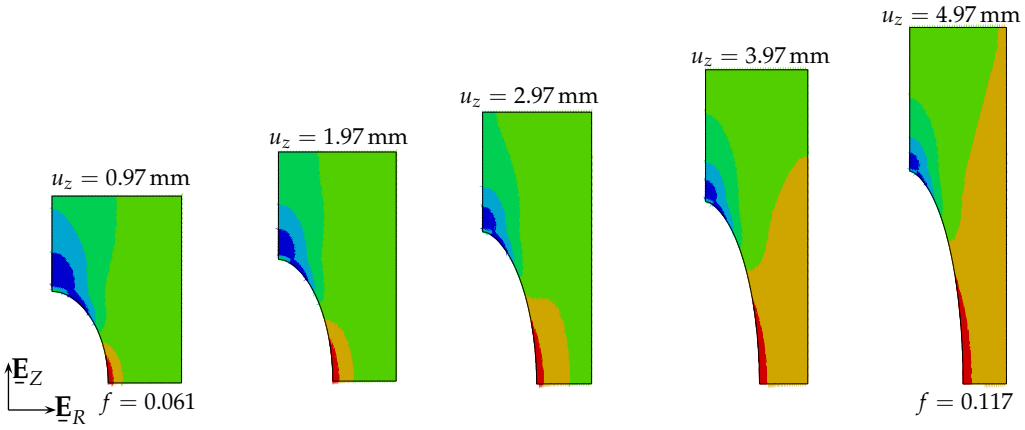

Figure 6: Deformation of the RVE model and evolution of contours of the lagrangian strain component LE_{22}. The initial porosity is $f_o = 0.050$ and along the whole process of loading the triaxiality is kept constant: $\mathcal{T} = 1/3$ (pure tension).

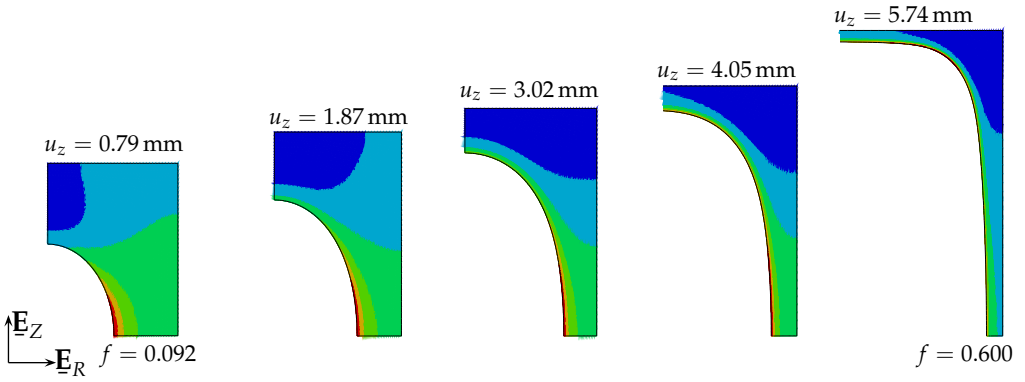

Figure 7: Deformation of the RVE model and evolution of contours of the lagrangian strain component LE_{22}. The initial porosity is $f_o = 0.050$ and along the whole process of loading the triaxiality is kept constant: $\mathcal{T} = 2$.

Figure 9 displays similar results as those shown in Fig. 5 for f_o ranging from 0.1 % to 10.0 %. It is to be noted that for $\mathcal{T} = 1$, each curve macroscopic equivalent stress versus macroscopic equivalent strains has a maximum depending on the initial value of the void volume fraction. Lower the initial value f_o of the void volume fraction, higher the reached value of the relevant peak stress. Table 1 shows the obtained associated values of $\left(\frac{\Sigma_e}{kT}\right)^{max}$, E_e, f, and the imposed axial displacements u_Z for $f_o = 0.1$, 0.5, 1.0, 2.0, 5.0 and 10.0 %. Beyond macroscopic peak stresses, the void volume fraction rapidly

increases. In this connection, it should be kept in mind that special care would be considered after maximum load occur in the vicinity of the boundary of void. Indeed, it is well known that strong softening of the material result in localized deformation and consequently the mesh size dependence. After the peak macroscopic stresses the equivalent stress drops abruptly and the validity of the numerical results is expected to quickly deteriorate because of mesh excessive distortion. In addition, it should be important to keep in mind that for the analysis presented above a criterion for the final failure of the intervoid ligament is clearly missing.

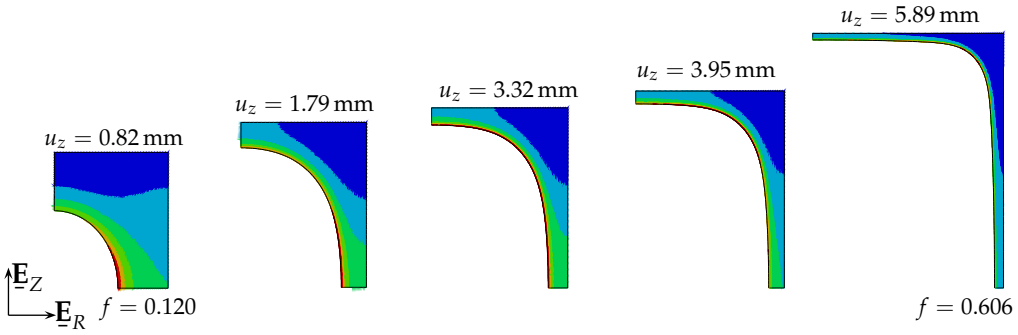

Figure 8: Deformation of the RVE model and evolution of contours of the lagrangian strain component LE_{22}. The initial porosity is $f_o = 0.050$ and along the whole process of loading the triaxiality is kept constant: $\mathcal{T} = 2$.

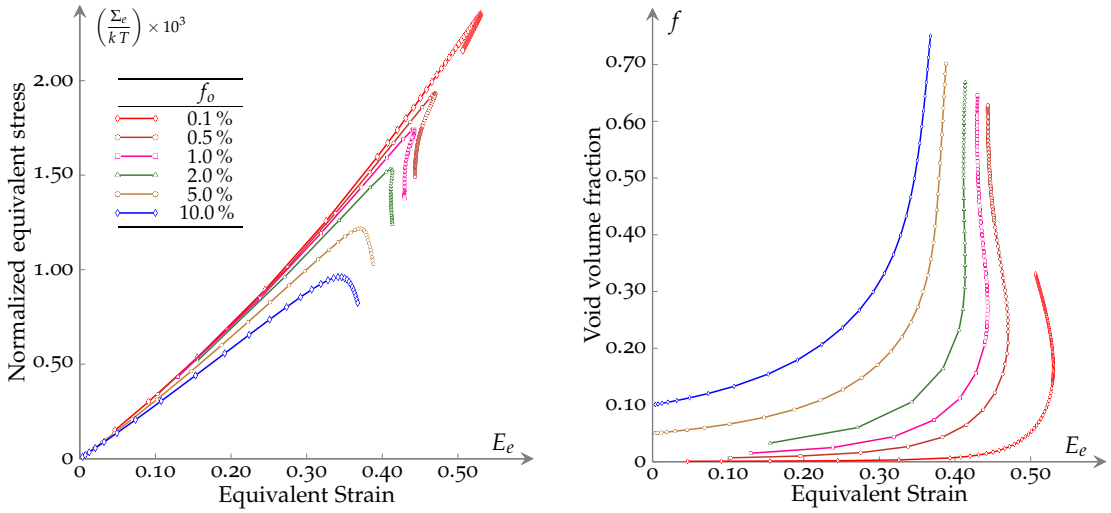

Figure 9: Evolution, for $\mathcal{T} = 1$, of the normalized effective stress and the void volume fraction in terms of the macroscopic effective strain E_e of the RVE model.

Table 1: Normalized maximum macroscopic equivalent stresses $\left(\frac{\Sigma_e}{k\,T}\right)^{max}$ and the corresponding macroscopic equivalent strain E_e, void volume fraction f, and axial displacements u_Z. The stress triaxiality $\mathcal{T}$ is equal to 1.

f_o (%)	$\left(\frac{\Sigma_e}{k\,T}\right)^{max}$	f (%)	E_e	u_Z (mm)
0.1	2.35×10^{-3}	15.8	0.53	2.75
0.5	1.93×10^{-3}	20.9	0.47	2.50
1.0	1.74×10^{-3}	23.9	0.44	2.40
2.0	1.53×10^{-3}	26.9	0.41	2.23
5.0	1.22×10^{-3}	38.6	0.37	2.33
10.0	0.96×10^{-3}	46.7	0.34	2.32

5 CONCLUDING REMARKS

This study focuses on the mechanical behaviour of porous polymeric gels intended for use in tissue engineering and regenerative medicine as scaffolds. Following Hong *et al.* [20] and Koplik and Needleman [24], we present a computational framework for investigating the growth of microvoids initially assumed to be spherical and uniformly distributed inside the matrix material. The evolution of the size and the shape of the microvoid has been obtained under the conditions that i) the ambient chemical potential of the solvent is fixed, ii) the chemical equilibrium prevails at the interface between the polymer and the environment interface, and iii) the mechanical loading of the RVE is such that the stress triaxiality ratio is maintained constant throughout the whole process of deformation. The following conclusions are drawn:

- For a porous polymeric gel, the amount of solvent molecules inside the material is related to the chemical potential of the environment. The degree of swelling is obtained by solving equations that account for the simultaneous interaction of mechanics and absorption. It can be determined with a free swelling stretch, using a finite element analysis.
- As an expected result, the value of the initial void volume fraction has a large influence on the overall mechanical behaviour of a porous polymeric gel. Higher the initial value of the void volume fraction, lower the resistance (maximum equivalent stress) of the polymeric gel.
- The size of the swollen axisymmetric porous RVE model does not depend on the initial value of the void volume fraction and the porosity is kept constant after

swelling.
- For moderate stress triaxiality, *e.g.*, $\mathcal{T} = \frac{1}{3}$, the macroscopic equivalent stress continuously increases with macroscopic equivalent strain. The same applies to the variations of the void volume fraction.
- For high stress triaxiality, the curves macroscopic equivalent stress *vs* macroscopic equivalent strain display maximum depending on both the initial porosity and the fixed value of the overall triaxiality.
- Finally, so far for the analysis presented above a criterion for the final failure of the intervoid ligament is clearly missing.

The investigation of the effects of the constitutive parameters entering the theory, namely, the number N of polymer chains per unit volume of the dry polymers, the volume per solvent molecule v, and the Flory interaction parameter χ, on the overall behaviour of a porous polymeric gel are contemplated as a future research work. The fact of the matter is that this preliminary study could be of some relevance in regard to failure of responsive polymeric gels. Numerous tissues and organs are hydrogel-like in nature and several issues related to the mechanics of hydrogels remain open (a short list is given in the review [28]). With increment of biomedical applications, computational modelling to predict the performance of these biomaterials for use in regenerative medicine and tissue engineering proves to be a valuable aid in assisting understanding of the behaviour of hydrogels and their optimization as well.

REFERENCES

[1] Artmann, G.M. and Chien, S. (eds) *Bioengineering in Cell and Tissue Research.* Springer, Heidelberg, Berlin, (2008).

[2] Baek, S. and Srinivasa, A.R. *A thermo-mechanically coupled theory for fluid permeation in elastomeric materials: Application to thermally responsive gels. International Journal of Nonlinear Mechanics* (2004) **39**:201-2018.

[3] Baek, S. and Pence, T.J. *Inhomogeneous deformation of elastomer gels in equilibrium under saturated and unsaturated conditions. Journal of the Mechanics and Physics of Solids* (2011) **59**:561-582.

[4] Ball, J.M. *Discontinuous equilibrium solutions and cavitation in nonlinear elasticity. Phil. Trans. Royal Soc., London. Series A* (1982) **306**:557-611.

[5] Brocks, W. Sun, D.Z. and Hönig, A. *Micromechanics of coalescence in ductile fracture. International Journal of Plasticity* (1995) **11**:971-989.

[6] Chester, A.S. and Anand, L. *A thermo-mechanically coupled theory for fluid permeation in elastomeric materials: Application to thermally responsive gels. Journal of the Mechanics and Physics of Solids* (2011) **59**:1966-2006.

[7] Disher, D. *et al.*, *Biomechanics: Cell research and applications for the next decade. Annals of Biomedical Engineering* (2009) **37**:847–859.

[8] Doi, M. *Gel dynamics. Journal of the Physical Society of Japan* (2009) **78**:052001-1–052001-19.

[9] Doi, M. *Soft Matter Physics.* Oxford University Press, Oxford, (2013).

[10] Dormieux, L. Kondo, D. and Ulm, F.-J. *Microporomechanics.* John Wiley & Sons, Ltd., Chichester, (2006).

[11] Duda, F.P. Souza, A.C. and Fried, E. *Theory for species migration in a finitely strained solid with application to polymer network swelling. Journal of the Mechanics and Physics of Solids* (2010) **58**:515-529.

[12] Duda, F.P. Souza, A.C. and Fried, E. *Solvent uptake and cavitation. Journal of the Mechanics and Physics of Solids* (2011) **59**:2341–2354.

[13] Fernandes, P.R. and Bártolo, P.J. (eds), *Tissue Engineering: Computer Modeling, Biofabrication and Cell Behavior.* Springer, Dordrecht, Heidelberg, (2014).

[14] Fish, J. *Practical Multiscaling.* John Wiley & Sons Ltd., Chichester, (2014).

[15] Flory, P.J. and Rehner, J. *Statistial mechanics of cross-linked polymer networks II. Swelling.* textitJ. Chem. Phys. (1943 **11**:521-526.

[16] Fond, C. *Cavitation criterion for rubber materials: a review of void-growth models. Journal of Polymer Science B: Polymer Physics* (2001) **33**:2081-2096.

[17] Foster, A.A. Marquardt, L.M. and Heilshorn, S.C. *The diverse roles of hydrogel mechanics in injectable stem cell ... Current Opinion in Chemical Engineering* (2017) **15**:15-23.

[18] Gent, A.N. and Lindley, P.B. *Internal rupture of bonded rubber cylinders in tension. Proc. R. Soc. Lond. A* (1959) **249**:195-205.

[19] Holzapfel, G.A. and Ogden, R.W. (eds) *Mechanics of Biological Tissue.* Springer, Berlin, Heidelberg, (2006).

[20] Hong, W. Liu, Z.S. and Suo Z.G. *Inhomogeneous swelling of a gel in equilibrium with a solvent and mechanical load. International Journal of Solids Structures* (2009) **46**:3282-3289.

[21] Horgan, C. O. and Polignone, D. A. *Cavitation in nonlinearly elastic solids: A review. Appl. Mech. Rev.* (1995) **48**: 471-485.

[22] Kang, M.K. and Huang, R. *A variational approach and finite element implementation for swelling of polymeric hydrogels under geometric constraints. Journal of Applied Mechanics* (2010) **77**:061004.

[23] Koh, C.T. Strange, D.G.T. Tonsomboon, K. and Oyen, M.L. *Failure mechanisms in fibrous scaffolds. Acta Biomaterialia* (2013) **9**:7326-7334.

[24] Koplik, K. and Needleman A. *Void growth and coalescence in porous plastic solids. International Journal of Solids Structures* (1988) **24**:835-853.

[25] Lefèvre, V. Ravi-Chandar, K. and Lopez-Pamies O., *Cavitation in rubber: an elastic instability or a fracture phenomenon? International Journal of Fracture* 2015) **192**:1-23

[26] Li, H. *Smart Hydrogel Modelling.* Springer, Dordrecht, (2009).

[27] Zheng, X. Li, S. and Kohles, S.S. *Multiscale Biomechanical Modeling of Stem Cell-Extracellular Matrix Interactions.* in: S. Li and B. Sun, (eds.), *Advances in Cell Mechanics, Chapter 2* Springer, Heidelberg, (2011):27-53.

[28] Liu, Z.S. Toh, W. and Ng T.Y. *Advances in mechanics of soft materials: large deformation behavior of hydrogels. International Journal of Applied Mechanics* (2015) **7**:35.

[29] Lopez-Pamies, O. *Onset of cavitation in compressible, isotropic, hyperelastic solids. Journal of Elasticity* (2009) **94**:115-145.

[30] Lopez-Pamies, O. *An exact result for the macroscopic response of particle-reinforced Neo-Hookean solids. Journal of Applied Mechanics* (2010) **77**:021016-1-021016-5.

[31] Ma, P.X. *Scaffolds for tissue fabrication. Materialstoday* (2004) **7**:30-40.

[32] Mauli Agrawal, C. Ong, J.L. Appleford, M.R. and Mani, G. *Introduction to Biomaterials.* Cambridge University Press, Cambridge UK, (2014).

[33] Migliaresi, C. and Motta, A. (eds) *Scaffolds for Tissue Engineering. Biological Design, Materials, and Fabrication.* Pan Stanford Publishing Pte. Ltd., Singapore, (2014).

[34] Nemat-Nasser, S. and Hori, M. *Micromechanics: overall properties of heterogeneous materials.* North-Holland, Elsevier, Amsterdam, 2nd edition, (1999).

[35] Pence, T.J. and Tsai, H. *Swelling-induced cavitation of elastic spheres. Mathematics and Mechanics of Solids* (2006) **11**:527-551.

[36] Rajagopal, K.R. *Diffusion through polymeric solids undergoing large deformations. Materials Science and Technology* (2003) **19**:1175-1180.

[37] Stella, J.A. D'Amore, A. Wagner, W.R. and Sacks, M. S. *On the biomechanical function of scaffolds for engineering load-bearing ... Acta Biomaterialia* (2010) **6**: 2365-2381.

[38] Treloar, L.R.G. *The Physics of Rubber Elasticity.* Oxford University Press, Oxford (1975).

[39] Volokh, K. *Mechanics of Soft Materials.* Springer, Singapore (2016).

[40] Wong, W.H. *Instability study of soft materials-Modelling and simulation.* PhD thesis, National University of Singapore, Singapore, (2011).

[41] J.A. Zimberlin, G.N. Tew, N. Sanabria-Delong, A.J. Crosby, *Cavitation rheology fo soft materials. Soft Matter* (2007) **3**: 763-767.